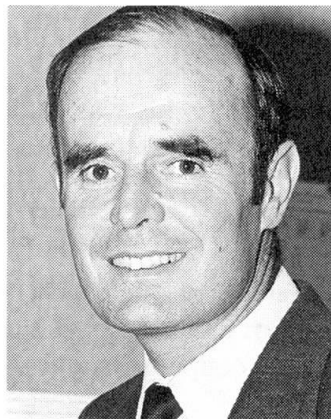# KEYNOTE SPEAKER

Evaluation of Reserve Capacity of Frames
Détermination de la réserve de capacité portante des cadres
Bestimmung der Tragreserve von Rahmen

Alan R KEMP
Prof. of Civil Eng.
Univ. of the Witwatersrand
Johannesburg, South Africa

Alan Kemp obtained BSc & MSc degrees in civil engineering from the University of the Witwatersrand and PhD from Cambridge University. Before becoming Professor of Civil Engineering at the University of the Witwatersrand, he was Group Consulting Engineer of Dorman Long (Africa). He is a past President of the S A Institution of Civil Engineers.

SUMMARY

Twin algorithms are described for separating linear and nonlinear moment-curvature characteristics of sub-members and then using these characteristics in elastic-plastic frame analysis with two submembers per frame member. Provision is made for complete stress-strain curves, residual stresses, shrinkage, plastic local and lateral buckling, interface slip and combinations of permanent and imposed load properties, as well as end connection flexibility. An example shows the enhanced ultimate load capacity that can be achieved in continuous structures and the required rotations of plastic hinges that are checked using a limit states criterion of ductility.

RÉSUMÉ

L'auteur expose des algorithmes doubles en vue de séparer les rapports courbures-moments de types linéaires et non linéaires dans les éléments porteurs secondaires, puis d'appliquer ces caractéristiques au calcul élastoplastique de cadres à deux éléments porteurs secondaires. Cette méthode prend en compte la totalité des diagrammes contrainte-déformation, les contraintes résiduelles, le retrait, le voilement et déversement local plastique, les surfaces de contact à glissement, la variation des propriétés sous charges permanente et utile, ainsi que la flexibilité des assemblages bout à bout. Un exemple met en valeur, d'une part l'augmentation de la charge portante ultime de structures hyperstatiques et, par ailleurs, les relations requises par les rotules plastiques qui sont vérifiées à l'aide d'un critère de ductilité à l'état ultime.

ZUSAMMENFASSUNG

Es werden Zwillingsalgorithmen zur Trennung der linearen und nichtlinearen Momenten-Krümmungsbeziehungen von Rahmenbauteilen mit zwei Untertraggliedern beschrieben. Sie berücksichtigen vollständige Spannungs-Dehnungskurven, Eigenspannungen, Schwinden, örtliches plastisches Beulen und Kippen, gleitende Kontaktflächen, Änderung der Eigenschaften unter Dauer- und Verkehrslast, sowie Nachgiebigkeit der Endverbindungen. Ein Beispiel belegt die gesteigerte Grenztragfähigkeit statisch unbestimmter Tragwerke und die benötigte Rotationsfähigkeit der plastischen Gelenke, die mit einem Duktilitätskriterium überprüft werden.

1. INTRODUCTION

Structural frames often possess load-resisting capacity above that assessed in the original design due to the following reasons:

- Semi-rigid end-connections that may provide continuity where simple-supports were assumed.
- Stress-strain properties of materials, including nonlinear effects, that differ from those originally assumed (conservative properties and partial material factors may be adjusted after in-situ testing).
- Partial composite action in structures where this was neglected.
- Benefits of limit states design codes allowing for redistribution of moments and ultimate (stress-block) resistances compared to older allowable stress codes, but also requiring more comprehensive analysis including non-linear P-Δ effects and ductility criteria.

If adequate analysis procedures are available, these factors will often lead to an assessed increase in load capacity. This may be improved further by strengthening procedures that enhance flexural resistance and stiffness, introduce additional continuity and load paths, or prevent secondary modes of strain-weakening behaviour.

The first two sections of this paper describe moment-curvature and frame analysis algorithms that link together to provide a computational method of allowing for all these nonlinear characteristics without the need for finite-element analysis involving numerous elements both across the sections and along the length. Features of this approach include:

1. In the frame analysis each "member" is represented by only two "sub-members", each reflecting the integrated non-linear behaviour between an end and the internal section of maximum moment (or the midspan if no maximum internal moment exists), without further discretization in inelastic regions.
2. The frame analysis identifies not only the ultimate load capacity, but also the plastic rotations at each critical section before loss of moment resistance, that are required to check the ductility, as described in the third section of the paper.
3. The behaviour of each element in positive and negative bending is determined in the moment-curvature algorithm allowing for nonlinear material behaviour, shrinkage, creep, interface slip, residual stresses and other effects.
4. This moment-curvature algorithm minimises the number of "elements" representing the cross-section because it is not necessary to subdivide for strain gradient through the depth.
5. Strain-hardening followed by strain-weakening behaviour beyond the elastic region is represented by an idealised elastic-perfectly-plastic moment-curvature relationship for frame analysis, together with expressions for determining the available plastic rotation prior to the moment falling below the design resistance.

The moment-curvature and frame analysis algorithms and the limit states criterion for ductility are illustrated by the example of a three-span composite beam in Fig. 1. Although this is a relatively simple structure, the approach has been applied to more complex sway structures involving frame instability [1,2]. This example is also used at the end of the paper to illustrate the reserve capacity that can be mobilised by allowing for nonlinear characteristics, including continuity in a previously simply-supported beam using the semi-rigid end detail reflected in Figs. 1b and c.

2. MOMENT/CURVATURE-ROTATION-DEFLECTION RELATIONSHIPS

2.1 Stress-strain models of material behaviour

Beam spacing = 2.5m
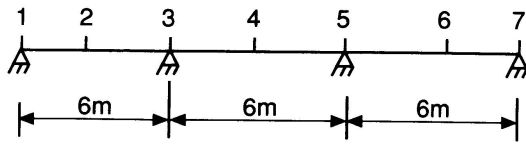
a) 3 - span beam : converted to
continuous composite beam.

b) Section dimensions

The moment-curvature method described in this paper has its origins in some of the many stress-strain models that exist [3], but has been developed and tuned progressively over the last decade by the author to represent consistently the inelastic behaviour of a wide range of structural components. Importantly, the results may be integrated to determine the element properties required for nonlinear frame analysis, including the assessment of required ductility using a mixed method of analysis that is described in the next section.

Any stress-strain curve is subdivided into three regions as illustrated in Fig. 2. Each region is represented by a local curve with an origin at the start of the region and a relationship in region i of the following form:

$$\Delta\sigma_i = E_i\Delta\varepsilon_i + D_i(\Delta\varepsilon_i)^{n_i} \tag{1a}$$

$$\Delta\varepsilon_i = \varepsilon - \varepsilon_{io} \tag{1b}$$

c) End connection M - θ curve

Fig.1 Composite beam example

which $\Delta\sigma_i$ and $\Delta\varepsilon_i$ are the changes of stress and strain at strain ε from the origin of the region, ε_{io} is the strain at the origin, E_i is the slope of the stress-strain curve at the origin and D_i and n_i model the observed characteristics of the material.

The general Eqns. 1a and 1b for each of the three regions are particularly useful in calculating the moment-curvature relationship because at any extreme fibre strain ε the average stress under the curve $\bar{\sigma}$, the location of the centroid of this area $c = \int\sigma\varepsilon d\varepsilon/\sigma\varepsilon^2$ and the tangental slope E_t may be expressed in simple algebraic form as follows:

Fig.2 Stress-strain curves

$$\bar{\sigma} = \sum_i A_i / \varepsilon \tag{2a}$$

$$A_i = \sigma_{io}\Delta\varepsilon_i + E_i\Delta\varepsilon_i^2 / 2 + D_i(\Delta\varepsilon_i)^{n_i+1} /(n_i+1) \tag{2b}$$

$$c = \frac{\sum_i [A_i\varepsilon_{io} + \sigma_{io}\Delta\varepsilon_i^2 / 2 + E_i\Delta\varepsilon_i^3 / 3 + D_i(\Delta\varepsilon_i)^{n_i+2}/(n_i + 2)]}{\bar{\sigma}\varepsilon^2} \tag{2c}$$

$$E_t = E_i + n_iD_i(\Delta\varepsilon_i)^{n_i-1} \tag{2d}$$

in which the summation extends over all regions i up to and including the region containing the strain ε, σ_{io} is the stress at the start of the region and A_i is the area under the stress-strain curve in any region given by Eqn. 2b. The index n_i is calculated from a known change of slope (E_t - E_i) over $\Delta\sigma_i$ and $\Delta\varepsilon_i$ from Eqns. 1a and 2d:
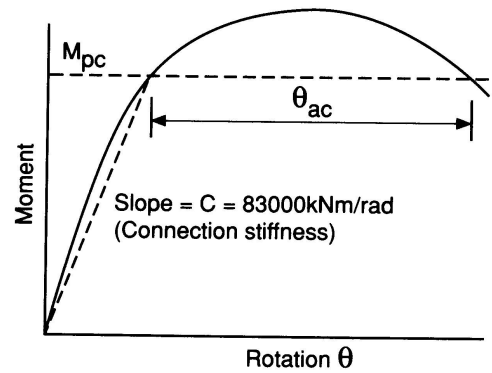
$$n_i - (E_i - E_t) \Delta\varepsilon_i / (E_i\Delta\varepsilon_i - \Delta\sigma_i) \qquad (2e)$$

The material properties that need to be specified to determine the unknowns E_i, D_i and n_i in the three regions of the curve apart from continuity are shown in Fig. 2 and Table 1. This table also includes in brackets typical design values, incorporating partial material factors, that are used in the example of Fig. 1.

2.2 Moment-curvature relationships

Any cross-section of a structural element comprising one or more materials and subjected to bending with or without coincident axial force, may be subdivided into an appropriate number of equivalent rectangular elements or concentrated areas to represent the geometry of the cross-section. This subdivision does not have to be sufficiently fine to neglect the strain gradient because of the availability of expressions for average stress and lever-arm of the resultant force vector given by Eqns. 2a to 2c. Thus a steel I-section may be represented by three equivalent rectangles and a reinforced concrete beam by one rectangle and one concentrated area, whereas a circular cross-section may require twelve rectangular elements.

A linear distribution of longitudinal strain is considered through the depth of the section and the strain gradient is assumed equal to the curvature. Considering any rectangular element j shown in Fig. 3 of breadth b, thickness t and depth of centroid y_c from an arbitrary reference level (the top surface), the axial force supported by the element and its moment of resistance may be determined directly from the stress-strain properties of the material described previously. The resistance of the rectangle under consideration ABCD may be represented by the difference in resistance of the rectangles ABEF and CDEF in this figure. For the strain distribution shown, representing a curvature or strain gradient ϕ:

Material (Fig.2)	Mod. of Elasticity E	Proportional limit f_p	Strain hardening/weakening	
			Onset	Slope
1. Structural Steel	(206 GPa)	$f_p = f_y$ ($f_y = 235$MPa)	$\varepsilon_s = (5\text{-}15)\varepsilon_y$ ($\varepsilon_s = 10\varepsilon_y$)	$E_s = E/(30\text{-}100)$ ($E_s = E/100$)
2. Metal (reinforcing)	(200 GPa)	$f_p = 0.8f_y$ ($f_y = 390$MPa)	$\varepsilon_s = (1.5\text{-}2)f_y/E$ ($\varepsilon_s = 2f_y/E$)	$E_s = E/(30\text{-}200)$ ($E_s = E/200$)
3. Concrete (Compression)	$E = 20\text{-}35$GPa ($E = 24$GPa)	$f_p = (0.5\text{-}0.8)f_c$ $f_c = 15$MPa $f_p = 9$MPa	$\varepsilon_m @ f_c =$ $0.002\text{-}0.0025$ ($\varepsilon_m = 0.0022$)	$E_s = -E/(3\text{-}50)^*$ ($E_s = -E/5$)
4. Concrete (tension)	E as for compression	$f_p = f_t = 0.3(f_c)^{2/3}$ $f_p = 1.8$MPa	$\varepsilon_s = (3\text{-}8)f_p/E$ ($\varepsilon_s = 4f_p/E$)	$E_s = 0$

* Depends on extent of triaxial restraint provided by reinforcement

Table 1. Material properties for stress-strain curves in Fig. 2

$$\varepsilon_u \cdot \phi y_u - \phi (y_c - 0,5t - y_n) \qquad (3a)$$

$$\varepsilon_l - \phi y_l - (y_c + 0,5t - y_n) \qquad (3b)$$

in which y_u and y_l are the depths from the neutral axis to the upper and lower surfaces of the rectangle defined as positive below the neutral axis, ε_u and ε_l are the corresponding strains and y_n is the depth of the neutral axis below the reference level.
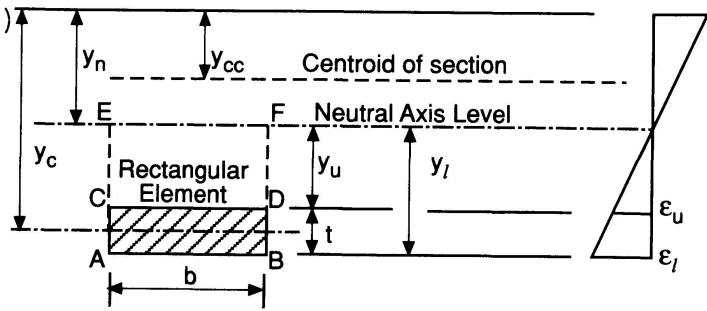

Fig.3   Assessment of element ABCD

The axial force F_j supported by element j is given by the difference in axial forces on the two rectangles ABEF and CDEF:

$$F_j - b \, (\overline{\sigma}_l y_l - \overline{\sigma}_u y_u) \qquad (4)$$

in which $\overline{\sigma}_l$ and $\overline{\sigma}_u$ are the average stresses under the stress-strain curve given by Eqns. 2a and 2b at strains ε_l and ε_u respectively.

The moment of resistance M_j of the element about the centroid of the complete section is given by the difference in moments of resistance of the two rectangles ABEF and CDEF:

$$M_j - b \, (\overline{\sigma}_l c_l y^2_l - \overline{\sigma}_u c_u y^2_u) + F_j \, (y_n - y_{cc}) \qquad (5)$$

in which c_l and c_u are the centroidal ratios given by Eqn. 2c and y_{cc} is the depth of the centroid of the section from the reference level. Similar expressions may be derived for concentrated areas such as reinforcement [4].

In all of the above equations the assumed sign convention is stress, strain and force positive in tension, curvature and moment positive in sagging bending and depth y positive below the arbitrary reference level. The expressions apply whether the element is above or below or cut by the neutral axis. For materials such as concrete the form of these equations also enables different stress-strain curves to be adopted under compression and tension by referring $\overline{\sigma}_l$, c_l and $\overline{\sigma}_u$, c_u to the properties of different materials if the neutral axis falls within the depth of the element.

In Eqns. 3 to 5 it is assumed that the depth of the neutral axis below the reference level y_n is known. At inelastic levels of stress and strain, y_n is determined iteratively to satisfy equilibrium between the net axial force resisted by the section, $\sum F_j$, and the external axial load N applied to the section.

The method has been applied [4] to a wide range of structures and elements of different materials at serviceability and ultimate load and has been adapted to model the following important aspects of structural behaviour:

● Prestressing and shrinkage in concrete elements, by introducing initial values of strain in the relevant elements.

● Residual rolling or welding stresses, by providing additional elements with different initial strains to reflect the residual stresses approximately, based on proposals such as Young [5].

● Interface slip in composite beams with partial shear connection, by introducing slip-strain increments at the interface that are a function of curvature and, when integrated over the half-

span of the beam, provide a total end slip that is consistent with measured behaviour in push-out or beam tests.

- A combination of differing section configurations and stress-strain properties under permanent and imposed loads.
- Strain-weakening due to interactive local and lateral buckling of yielded steel sections based on a semi-empirical model described by Kemp [6].

2.3 Idealisation for frame analysis

The moment-curvature relationships for the composite beam example shown in Fig. 1b, with material properties defined in brackets in Table 1, are illustrated by the solid lines in Fig.4 for positive and negative bending. The ultimate design resistance M_p is an important parameter that is determined from code rules in this case, or other considerations. These curves include the effects of residual rolling stresses, interface slip due to a 50% partial shear connection and interactive plastic local and lateral buckling at high moments in the negative moment region. The region of the beam adjacent to the semi-rigid end connection shown in Figs. 1b and c has been modelled by assuming that the steel section cannot resist tension.

In the three-span continuous beam of Fig 1a, the first regions to develop plastic hinges are adjacent to the internal supports. Uncertainty exists over the moment-curvature path followed by sections in the inelastic region adjacent to these supports (represented by portion PM in Fig. 4b) once the structure is loaded under displacement control beyond the maximum moment and experiences strain-weakening with the section of maximum moment following portion MM' in Fig. 4b. Based on a qualitative assessment of test behaviour it is proposed that the distribution of curvature in this inelastic region at the load level at which the maximum moment at the internal support falls to the design resistance M_p may be modelled simply and approximately by the line P'M'. This implies that curvature is a linear function of moment and the available inelastic rotation θ_{ap} is given by the shaded area in Fig. 4b as:

$$\theta_{ap} - 0.5M_p \ (m \ -1) \ [\phi'_m - \phi_p \ (m \ +1) \ / \ 2m]/mV_p \qquad (6)$$
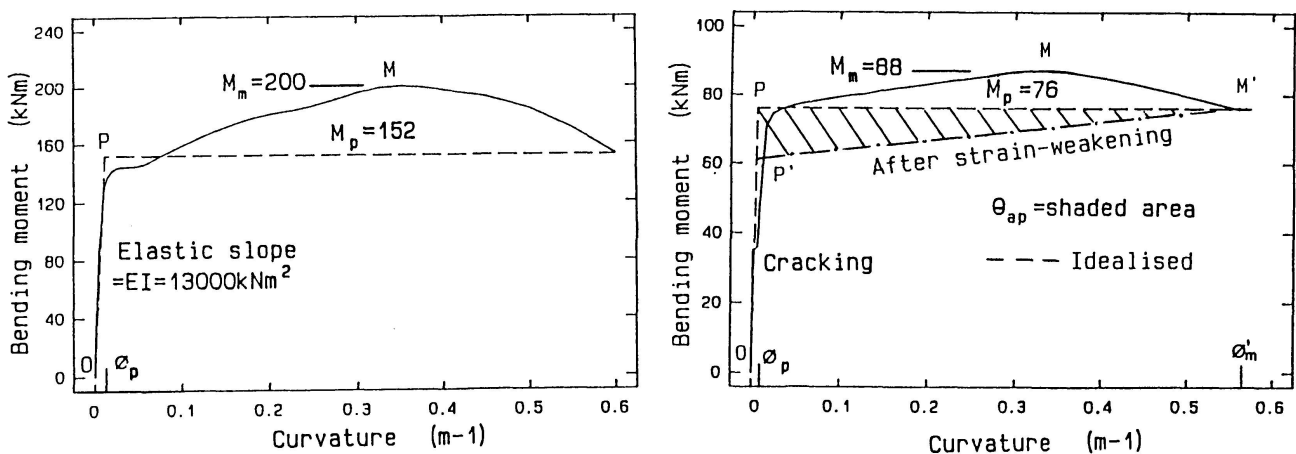
a) Positive (sagging) bending   b) Negative (hogging) bending

Fig. 4 Moment-curvature relationships for example of Fig. 1

in which V_p is the shear force at the section of maximum moment and $m = M_m/M_p$ in Fig. 4b.

On this basis the behaviour of elements of the structure between sections of zero moment and adjacent sections of maximum positive or negative moment (or adjacent joints) may be modelled in the frame analysis described subsequently as the superposition of the following effects:

1. Elastic behaviour is represented by the slope of the dashed elastic region of the idealised moment-curvature relationship OP in positive bending $EI = M_p/\phi_p$.
2. Inelastic behaviour is modelled by the horizontal dashed line PM' representing a concentrated ideally-plastic hinge of moment capacity M_p with an available rotation capacity θ_{ap} equal to the shaded area in Fig. 4b and given by Eqn. 6.
3. Differences in stiffness between positive and negative moment regions including cracking of concrete adjacent to internal supports, is represented by an additional component of available plastic rotation θ_{acr} given approximately by the integration of a linear difference in flexural rigidity between the positive moment EI and the cracked negative moment EI', as follows:

$$\theta_{acr} - \theta_e [1 - (M_{cr} / M_p)^2] [(EI / EI') -1] \qquad (7)$$

in which θ_e is the calculated elastic rotation in the negative moment region and M_{cr} is the moment at which cracking occurs.

4. Semi-rigid end connections are represented by an idealised elastic stiffness C in Fig. 1c and, in cases where the connection rather than the adjacent member is the critical flexural element, by identifying the available plastic rotation θ_{ac} of the end connection prior to the moment falling below the design value M_p as shown in this figure.

3. FRAME ANALYSIS

3.1 Mixed flexibility/sway-deflection method

The selection and development of a mixed flexibility/sway-deflection method of analysis arose primarily from convenience in modelling elastic and inelastic behaviour, differences in negative and positive moment characteristics and semi-rigid connections, as outlined in the previous section [1,2]. By selecting end moments and independent sway-deflections as unknowns in frame analysis all of these properties including the development of plastic hinges can be considered on a consistent basis without changing the number or location of the unknowns. Additional benefits of this approach include:

- In nonlinear analysis the use of end moments as unknowns rather than joint displacements is likely to lead to more stable and sensitive solutions.
- Axial forces in members are determined from equilibrium considerations rather than as a stiffness function of axial distortions.
- The unknown independent sway-deflections are all directly related to the plastic and instability mode shapes of the structure and therefore relevant to inelastic P-Δ methods.

The method is described firstly in terms of the unknown end moments and then in terms of the additional unknown, independent sway-deflections.

3.2 Solution equations for unknown end moments

In the substructure shown in Fig. 5 that is used for illustrating this approach, ij is one of the two

sub-members representing member ijn between sections of maximum moment (or midspan if there is no internal section of maximum moment). The matrices relating end rotations θ to end moments M and relative end deflections due to sway δ_s (all positive anti-clockwise) in ij are:

$$\begin{pmatrix} \theta_{ij} \\ \theta_{ji} \end{pmatrix} = \frac{L}{EI} \begin{bmatrix} (b_1/3 + f) & -b_2/6 \\ -b_2/6 & (b_1/3 + f) \end{bmatrix} \begin{pmatrix} M_{ij} \\ M_{ji} \end{pmatrix} + \begin{pmatrix} \delta_{sij}/L \\ \delta_{sij}/L \end{pmatrix} \qquad (8)$$

in which L and EI are the length and elastic flexural rigidity of the member, b_1 and b_2 are Berry stability functions [7] that allow for increased flexibility due to axial force and have values of unity when second-order P-Δ effects are neglected and f is the non-dimensional flexibility ratio of the end connection expressed in terms of the elastic stiffness of the connection, C in Fig. 1c :

$$f = EI / CL \qquad (9)$$

The following equations are used for solving the n unknown moments at the ends of the n members meeting at joint i in Fig. 5a (n = 4 in Fig. 5a) :

1. One equation representing equilibrium of the moments, M at the ends of the members meeting at joint i:

$$\sum_1^m M_i = M_{ij} + M_{ik} + M_{il} + M_{im} = M_i' \qquad (10)$$

in which M_i' is the magnitude of any external moment applied to joint i.

2. (n-1) compatibility equations expressing the equality of rotations at the ends of each pair of members meeting a joint i (three compatibility equations for joint i in Fig. 5a representing equal rotations at end i of members ij and ik, ij and il, and ij and im), as follows:

$$\bar{\theta}_{ij} = \bar{\theta}_{ik} ; \quad \bar{\theta}_{ij} = \bar{\theta}_{il} \quad \text{and} \quad \bar{\theta}_{ij} = \bar{\theta}_{im} \qquad (11)$$

in which, for example in sub-member ij, $\bar{\theta}_{ij} = \theta_{ij} + \theta'_{ij} + \theta_{rij}$ and $\bar{\theta}_{ij}$ is the superposition of θ_{ij} (the end rotation due to unknown end moments given by Eqn. 8), θ'_{ij} (the end rotation due to member loads with end moments equal to zero - i.e. simply-supported) and θ_{rij} (the required plastic rotation of a hinge if it develops at this section, as discussed subsequently). In considering P-Δ effects the end rotations θ' may be amplified due to axial force using Berry functions [7].
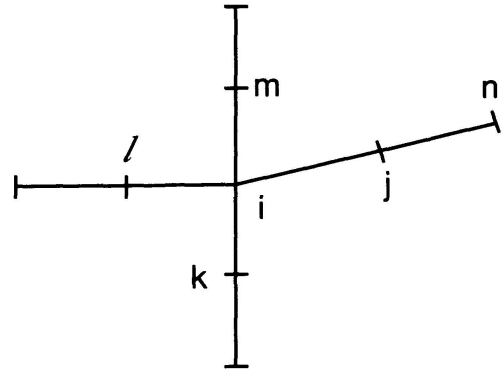
a) Substructure and sub - members
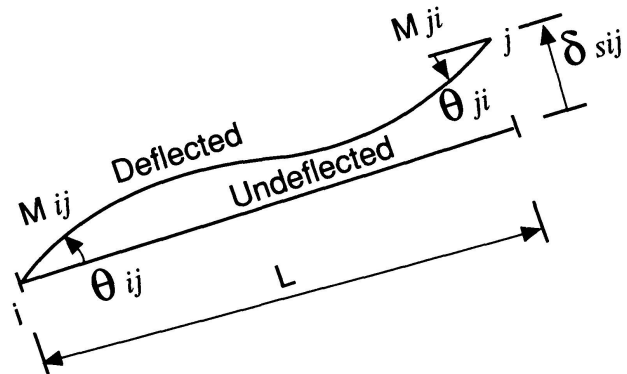
b) Sub - member ij

Fig.5   Sub-member ij at joint i

The only exception to this subdivision of equilibrium and compatibility equations occurs at a fixed support where all n equations will be compatibility equations.

3.3 Solution equations for unknown sway deflections

The independent modes of sway are treated as additional unknowns and the approach therefore becomes a mixed method combining unknown end moments with unknown independent sway deflections.

In a structure with j joints, m members and r constraints to global translation at support joints (horizontal and vertical components), there are s independent components of sway deflection given by:

$$s - 2j - m - r \qquad (12)$$

A systematic approach has been developed by the author [1] for identifying the most appropriate unknown joint translations to represent these s unknown modes of sway and their relationship to the other joint translations. Typically there is one mode of sway representing plastic collapse of each member and one representing each mode of sway instability. In this algorithm conventional sway-equilibrium equations are used to solve for each unknown sway deflection and are derived by the Principle of Virtual Displacements applied to a virtual free body displacement of the structure in the mode of sway. These sway equilibrium equations are expressed in terms of:
- the unknown end moments in the sub-members,
- P-Δ terms for elastic or inelastic stability analysis in which P are the axial forces extrapolated from the previous iteration and Δ are the unknown sway deflections normal to P.

3.4 Application of this frame analysis method

This mixed flexibility/sway-deflection method may be used in the same form for elastic, elastic-plastic and elastic-plastic-instability (P-Δ) analyses as follows:
1. Elastic analysis (including elastic connection flexibility) : The unknown end moments are solved using the idealised (dashed) elastic properties in Fig. 4a and the joint equilibrium and compatibility Eqns. 10 & 11 and the unknown sway deflections using conventional sway-equilibrium equations.
2. Elastic-plastic analysis : After the elastic analysis, plastic hinges may be introduced at critical sections either by defining the ultimate design resistance M_p or by identifying a specified ratio between the moment capacities at two sections and the location at which a hinge is expected to develop. In either case the moment at the plastic hinge is then known and is replaced as unknown by the required plastic hinge rotation θ_r (forming part of Eqn.11) to accommodate the necessary redistribution of moments, as discussed subsequently.
3. Elastic-plastic-instability and P-Δ analyses : The elastic-plastic analysis approach is extended to include the Berry stability functions in Eqns. 8 & 11 and the P-Δ term in the sway-equilibrium equations. The member axial force is extrapolated from the previous analysis step introducing a limited iterative procedure.

4. REMAINING CAPACITY ASSOCIATED WITH REDUNDANCY

A significant source of reserve or remaining capacity may exist in redundant structures if they possess sufficient ductility to redistribute moments from heavily stressed sections, at which the

ultimate stress-block moment M_p is achieved, to less heavily stressed sections as the load is increased. The two preceding parts of this paper have described relatively simple algorithms for determining results that are directly relevant to assessing ductility, namely:

1. The available inelastic rotation θ_a at plastic hinges prior to the moment falling below the ultimate resistance M_p and made up of components due to plastic behaviour θ_{ap} (Eqn. 6), inelastic rotation of end connections θ_{ac} (Fig. 1c) and reduced stiffness due to cracking of negative moment regions, θ_{acr} (Eqn.7).

2. The required inelastic rotation θ_r at the same plastic hinges from the frame analysis of the redundant structure for specified loads and ultimate resistances M_p.

A general limit states criterion of ductility has been proposed [2] for determining how much capacity exists in indeterminate structures to redistribute moments. This requires that the available inelastic rotation θ_a at each plastic hinge should be greater than the plastic rotation θ_r required to achieve the specified level of moment redistribution or hinge development:

i.e. LIMIT STATE OF DUCTILITY : $(\theta_a / \gamma_{md}) > \theta_r$ (13)

in which γ_{md} is a partial material factor to allow for the considerable uncertainties in assessing θ_a and θ_r, in the range 1.5 to 3 depending on whether it is a ductile or brittle mode of failure. This criterion may be expressed non-dimensionally in terms of rotation capacity by dividing both sides by the elastic rotation at M_p between the plastic hinge and the adjacent section of zero moment. The criterion conforms to limit-states terminology by having a resistance on the left hand side and an action effect on the right hand side, and may be applied to any mode of failure inhibiting ductility for all types of structural materials.

5. EXAMPLE

Consider the three-span steel beam illustrated in Fig.1 that was originally designed as non-composite and simply supported with cleat connections only resisting shear, but is to be considered for upgrading into a continuous composite beam. The slab contained 0.4% longitudinal reinforcement over the internal supports for crack control and this will be utilised. The spans are about 2/3rds of a typical full-scale beam, but reflect the dimensions of a similar specimen tested by the author for available plastic rotation [8]. The nominal load carrying capacity of the existing beam is 6kN/m of permanent and 2 kN/m^2 of imposed load on the basis of an existing allowable stress code for steel, assuming the compression flange is restrained against lateral buckling.

Upgrading will be achieved by cutting out slots in the concrete above the steel beam to accomodate a partial shear connection capable of mobilising 50% of the ultimate slab force in sagging bending and the full effective area of reinforcement over the internal supports (500 mm^2). Each beam will be propped at midspan during casting of the grout around the shear connectors and welding of the end plate to the bottom flange of the steel beam and adjacent web as shown in Fig. 1b. This end plate provides a semi-rigid end connection with moment resistance made up of the reinforcement in tension and the bottom flange in compression when the prop is released [8].

The evaluation of the enhanced load-carrying capacity at the ultimate flexural limit state is undertaken as follows:

● The properties of rows 1 to 4 of Table 2 are determined using the moment-curvature results in Fig. 4 allowing for interactive plastic local and lateral buckling in negative bending and concrete crushing in positive bending.

- The properties in rows 5 and 6 of this table are calculated from these values using Eqns. 7 and 6 respectively.
- The elastic flexibility ratio f of the end connection (row 7) is determined from experimental results (Fig. 1c) using Eqn.9 : no significant nonlinear component of connection rotation was apparent at the level of moment developed in the adjacent member, so θ_{ac} = 0 in this case.
- An ultimate load capacity of the three-span beam of 41.8 kN/m associated with plastic hinges at the internal supports and midspan region of the outside spans, is determined from the frame analysis, in two steps (elastic and plastic) using 6 sub-members (Fig. 1a) and 12 unknown end moments and 3 unknown sway deflections. This represents a more than three-fold increase in the existing imposed load capacity of this beam.
- Required plastic hinge rotations in the outside spans adjacent to the internal supports θ_r = 0.0135 rad. are obtained from the frame analysis and are used as the action effect in Eqn. 13 to check the ductility involved in plastic moment redistribution. A partial material factor of γ_{md} = 1.5 is adopted for ductile failure due to local and lateral buckling and the resistance effect is the available plastic rotation θ_a = 0.0216 rad. made up of θ_{ac} (equal to zero), θ_{acr} and θ_{ap} (from Table 2, rows 5 and 6).

Limit States Criterion (Eqn.13) : (0.0216 / 1.5 > 0.0135)

The available plastic rotation θ_a compares favourably with tests on composite beams with similar semi-rigid end connections [8]. This excellent ductility is explained in this reference by the location of the plastic neutral axis being close to the compression flange which severely inhibits local and lateral buckling.

Moment-curvature properties (Fig.4) :	+ve Moment Region	-ve Moment Region
1. Elastic flexural rigidity EI (kNm^2) 2. Ultimate design resistance M_p (kNm) 3. Maximum moment M_m (kNm) 4. Falling branch curvature ϕ'_m (m^{-1})	13000 152 200	13000 (+ve moment) 76 (semi-rigid) 88 0.56
Assessed properties:		
5. Plastic rotation (Concrete cracking) θ_{acr} Eqn.7 (rad.) 6. Plastic rotation (yielding) θ_{ap} Eqn. 6 (rad.)	N/A N/A	0.0017 0.0199
Experimentally measured properties:		
7. Elastic flexibility ratio of end connection f = EI/CL (Eqn.9)	N/A	0.05

Table 2. Properties required for frame analysis

6. CONCLUSIONS

A significant source of reserve capacity exists in many structures if the implications of inelastic material behaviour, continuity and plastic redistribution of moments as well as the ductility requirements, can be assessed analytically without resorting to finite elements models that require

numerous elements both across the section of the members and along their length. A twin algorithm is illustrated in this paper for assessing firstly the inelastic section properties of two sub-members per frame member, and secondly the elastic-plastic-instability analysis of frames comprised of these sub-members. These analyses also identify the available and required plastic rotations that are used to check adequate ductility using a simple limit states criterion involving material plasticity, inelastic properties of end connections and differing flexural rigidities in positive and negative bending.

7. REFERENCES

1. KEMP A.R., A Consistent Mixed Approach to Computer Analysis of Frames. Civil Engineer in South Africa, 30(7), 317-322, July 1988.
2. KEMP A.R., Quantifying Limit States of Rotation Capacity in Flexural members. Proc. Institution of Civil Engineers, 89(2), 387-406, Sept. 1990.
3. DESAI C.S. and SIRIWARDANE H.J., Constitutive Laws for Engineering Materials. Prentice-Hall, New York, 1984.
4. KEMP A.R., Simplified Modelling of Material Non-Linearity in Structural Frames. Civil Engineer in South Africa, 30(9), 425-432, Sept. 1988.
5. YOUNG B.W., Residual Stresses in Hot-Rolled Sections. Dept. of Engin., Technical Report No. CUED/C - Struc/TR8, University of Cambridge, 1971.
6. KEMP A.R. and DEKKER N., Available Rotation Capacity in Steel and Composite Beams. The Structural Engineer, 69(5), 88-97, March 1991.
7. PIPPARD A.J.S. and BAKER J.F., The Analysis of Engineering Structures. 3rd Edition, Edward Arnold, London, 550-555, 1957.
8. KEMP A.R., TRINCHERO P. and DEKKER N., Ductility Effects of End Details in Composite Beams. Engineering Foundation Conference on Composite Construction, Potosi, Missouri, June 1992.